

DUST IN STAR-FORMING GALAXIES

Daniela Calzetti ¹

¹ *Space Telescope Science Institute, 3700 San Martin Drive, Baltimore, MD 21218, U.S.A.*

Abstract

I review the effects of dust obscuration in galaxies at both low and high redshifts, and briefly discuss a method to remove dust reddening from the emerging light of star-forming galaxies. I also analyze the evolution of the dust opacity in galaxies as a function of redshift, and discuss its effect on the observed UV-optical light. The quantitative corrections for dust obscuration given here allow one to recover the intrinsic value of the global star formation at different cosmological times.

1 Are Galaxies Opaque?

The general question is: how much of the light produced by all galaxies is absorbed by dust? Answering this question is crucial for understanding the evolution and the star formation history of galaxies. It is also an intrinsically difficult task, because: (1) dust is a source of continuous opacity and lacks readily recognizable signatures, such as absorption or emission features, in the UV-optical-nearIR regime; (2) the complex geometrical distribution of dust and stars affects both the global attenuation and the reddening of the emerging light from unresolved galaxies; (3) the colors produced by dust reddening and by age are often degenerate.

The geometry of the dust is the dominant factor which determines the appearance of a galaxy (Witt, Thronson, & Capuano 1992, Calzetti, Kinney & Storchi-Bergmann 1994, Witt & Gordon 1996). This is especially true when the galaxy is unresolved, and only its spatially integrated light can be measured. Large amounts of dust can be hidden by a clumpy distribution; if the dust clumps are small and compact, the interclump regions provide enough clear lines of sight that the galaxy will appear almost dust-free. An homogeneous mixture of dust and gas has a similar effect: the major contribution to the emerging light comes from the outermost layers of the galaxy, while the inner regions are generally opaque; the emerging spectral energy distribution then appears almost unreddened, but much dimmer than in the dust-free case. The total mass and stellar content of the galaxy will thus be underestimated by an amount which depends in a nonlinear fashion on the total dust content.

The absence of recognizable features has one exception: the 2200 Å “bump”, namely the broad UV absorption feature characteristic of the dust extinction in our Galaxy. The “bump”, however, cannot be used as a reliable gauge of the amount of dust in a galaxy. Its intrinsic depth is different in different galaxies, with the LMC extinction curve in the 30 Doradus region showing a shallower bump than the average Galactic extinction curve and the SMC extinction not showing a bump at all. The LMC and SMC are the only two external galaxies where accurate measures of interstellar reddening have been possible (see, however, Bianchi et al. 1996 for the case of M31). The bump even changes characteristics along different lines of sight

within the Milky Way itself (Cardelli, Clayton & Mathis 1989). The nature of the variability of the bump from galaxy to galaxy is not entirely clear, although it probably reflects variable grain size distributions and/or changing ratios in the dust ingredients as the characteristics of the local ISM and environment vary (see Gordon & Clayton 1998). Finally, even if the extinction curves were independent of the galaxy characteristics, the observed depth of the 2200 Å bump is a function not only of the total amount of dust along the line of sight, but also of the geometrical distribution of the dust relative to the emitters (Natta & Panagia 1984).

A dust reddened stellar population may resemble an “old” population. The dust-age degeneracy is an important effect when only broad band colors or low resolution spectroscopy are available for the object of interest and stellar features are not identifiable. In numbers: an optical attenuation $A_V=1$ changes the colors enough to mimic an age “increase” of a factor of ~ 5 in a stellar population less than 100 Myr old. Conversely, the colors of a relatively old stellar population will not be easily discriminated from the colors of a young but reddened population.

1.1 Opacity at Low Redshift

Given the difficulties listed above, different authors have taken different approaches to the problem of determining the opacity of galaxies in the local Universe.

The cleanest technique for measuring the dust opacity of a galaxy is the one which measures the obscuration produced by a foreground galaxy on background sources. The background sources can be either distant galaxies (Gonzalez et al. 1998) or another nearby galaxy overlapping with the first along the line of sight (e.g.: White, Keel & Conselice 1996, Berlind et al. 1997). With this technique, the light source is external to, and thus uncontaminated by, the galaxy for which the opacity is to be measured. Therefore, all complications due to the complex geometry of the dust inside the galaxy are circumvented, as the foreground galaxy acts as a dust screen in front of the background sources. To date, studies have concentrated on spiral galaxies as foreground objects. These have been shown to have transparent interarm regions, with $A_B \sim A_I \sim 0.1-0.2$, and opaque arms, with $A_B \sim A_I \sim 1$. As expected, the opaque regions of spirals coincide with the regions of most intense star formation (the arms), as stars form in the dusty molecular clouds. Using the variation of the galaxy surface brightness with inclination, Giovanelli et al. (1995) have shown that the same level of opacity as the arms is found in the centers of the spirals.

Another potentially powerful technique to determine the opacity of a galaxy is to measure the ratio between the UV-optical-nearIR stellar emission and the far-infrared (FIR) dust emission. This ratio represents the amount of stellar radiation which directly escapes the galaxy versus the amount of stellar radiation which has been absorbed by dust and is re-radiated in the FIR. The power of the method is that it relies uniquely on energy conservation. The shortcoming is that an accurate determination of the energy balance requires the sampling of the entire wavelength range from the far-UV to the far-IR, while, in general, only a few data points are available along the spectrum. A wealth of data exist for galaxies at optical, near-IR and, thanks to IRAS, in the 8-120 μm region, but only relatively recently UV measurements and FIR data beyond 120 μm are becoming available for large enough samples of galaxies. UV data are crucial for an accurate energy balance because the UV can be energetically dominant if recent star formation is present in the galaxy. Over the last couple of years, ISO has added data points in the 120-240 μm regime, covering another crucial wavelength regime: the one which contains the peak of dust emission from quiescent galaxies. Studies employing UV, optical, and IRAS data have concluded that in disk galaxies the amount of stellar light absorbed by dust and re-emitted in the FIR range is about the same as the emerging stellar light (Soifer

& Neugebauer 1991, Xu & Buat 1995, Wang & Heckman 1996). We have learned during this Conference that preliminary results from ISO observations indicate that about 30–50% of the UV emission from the CFRS galaxies is hidden by dust (Hammer 1998, these Proceedings).

Although none of the above results can be considered final, there is mounting evidence that galaxies in the local Universe are generally not very opaque. The available data currently suggest that dust absorbs $\sim 1/2$, and probably no more than $2/3$, of the total stellar light in local galaxies.

1.2 Opacity at High Redshift

At high redshift, the sampled wavelength baseline is more limited than at low redshift, as the rest-frame UV and optical range fall in the observed optical and IR range; thus determinations of opacities are even less secure than in the local Universe. One could expect dust opacity to be a minor issue at high redshift, as young galaxies were also metal-poor and, therefore, dust-poor. However, low metallicities were coupled with large gas column densities, which can in principle produce non negligible opacities. In addition, standard observing techniques target the rest-frame UV emission from high redshift galaxies, a wavelength range very sensitive to the obscuring effects of dust.

Meurer et al. (1997) have been among the first to raise the issue of dust opacity for the galaxy population at $z \sim 3$, by noticing that the UV spectral energy distributions of the Lyman-break galaxies (Steidel et al. 1996) are too red to be dust-free star-forming objects. They attempt a correction for dust reddening of the high redshift galaxies by extrapolating a method used for local starburst galaxies (Calzetti et al. 1994, Calzetti 1997), and conclude that on average $\sim 9/10$ of the UV light is lost to dust obscuration. Rowan-Robinson et al. (1997) use ISO to detect the FIR emission from distant galaxies in the Hubble Deep Field and conclude that about $4/5$ of the UV light at $z > 2$ is absorbed by dust. Near-IR spectroscopy of six of the Lyman-break galaxies has yielded measurements of the nebular emission lines in the rest-frame optical, which indicate that between $1/3$ and $1/6$ of the UV light escapes from the galaxies (Pettini et al. 1998; Pettini 1998, these Proceedings).

2 Is Dust Opacity Relevant for Dwarf Galaxies?

Dust formation is strictly linked to metal production. Thus, low metallicity systems, such as dwarf galaxies, are expected to contain little dust. Although observations confirm this to be a generally true statement, the global effect of the dust on the emerging light greatly depends on its geometrical distribution within the galaxy, as stated above.

The case of NGC5253 is enlightening in this respect. This dwarf galaxy, located in the Centaurus Group ~ 4 Mpc away from the Milky Way (Sandage et al. 1994), has a metallicity $\sim 0.1 Z_{\odot}$. HST images show NGC5253 as a bright UV emitter (e.g. Meurer et al. 1995, Calzetti et al. 1997), a consequence of the fact that the central region of the galaxy is undergoing a powerful burst of star formation. IRAS and other measurements, however, indicate that the galaxy's central region is also a bright far-infrared emitter, with a FIR luminosity comparable to the B-band emission of the entire galaxy. The FIR emission is a clear indicator of the presence of dust, and, in this case, of dust heated by the recently formed stars (Aitken et al. 1982). A detailed analysis of the reddening characteristics of the starburst in NGC5253 shows that about $2/3$ of the galaxy UV ($2,600 \text{ \AA}$) light is absorbed by dust (Calzetti et al. 1997). In conclusion, despite the fact that the galaxy is metal-poor and, therefore, should contain a small amount of dust, a non negligible fraction of its light is still lost to dust absorption. The galaxy

is nevertheless bright in the UV, a sign that the inhomogeneous distribution of dust produces a ‘picket-fence’ geometry, with ‘holes’ in the dust distribution through which the UV light can emerge.

3 Reddening in Actively Star-Forming Galaxies

The starburst regions of galaxies are characterized by high energy densities (e.g. Kennicutt 1989); massive star winds and supernova explosions inject energy into the ISM creating shock waves and gas outflows. Shocks from supernovae are most likely responsible for the destruction of dust grains, via grain-grain collisions and sputtering (Jones et al. 1994). Gas outflows can develop into “superwinds” (Heckman, Armus & Miley 1990) and eject significant amounts of the interstellar gas and dust from the site of star formation. As a result, the starburst environment is likely to be rather inhospitable to dust (Calzetti, Kinney & Storchi-Bergmann 1996).

If little diffuse dust is present within the starburst site, the main source of opacity is given by the dust *surrounding* the site. This dust is internal to the galaxy, but external (or mostly external) to the starburst region. This leads to a simplified description of the distribution of the dust affecting the starburst population: the geometry is equivalent to a dust shell surrounding a central light source. Such description is rather accurate for the reddening affecting the optical-nearIR nebular gas emission (Calzetti et al. 1996). Figure 1a plots the color excess $E_g(B-V)$ measured from two pairs of nebular line ratios, the widely used $H\alpha/H\beta$ and the long-baseline $H\beta/Br\gamma$, for a sample of starbursts. The two color excesses are sensitive diagnostics of dust geometry because of their difference in wavelength baseline. The data points of Figure 1a lay along the lines which identifies the homogeneous or clumpy screen dust models, while the other configuration, i.e. the homogeneous mixture of gas and dust, is excluded. An immediate consequence is that the color excess $E_g(B-V)$ measured from *any* pair of hydrogen recombination lines in the wavelength range (0.48–2.2 μm) is a reliable indicator of dust reddening for the gas in the starburst. It should be remarked that the screen model is an approximated description of the reddening affecting the nebular lines. For instance, dark and compact dust clumps within the starburst site are not excluded by the data.

If the *observed* stellar continuum colors are plotted as a function of $E_g(B-V)$, the two quantities correlate over the entire wavelength range 0.12–2.2 μm (Figure 2). This correlation spans a much wider range of colors than expected from variations of the intrinsic stellar populations in the starburst (see, e.g., the models by Leitherer & Heckman 1995). The most straightforward interpretation of the data in Figure 2 is that the stars are affected by a change in dust reddening proportionally to the way the ionized gas is affected. The reddening measured from the gas can then be used as the independent parameter to derive a “reddening curve” for the stellar continuum of starbursts (Calzetti et al. 1994; Calzetti 1997). The reddening curve is shown in Figure 1b and compared with the interstellar extinction curves of the Milky Way, the LMC and the SMC. However, the reddening curve is *not* an extinction curve. It is derived from the spatially integrated colors of the entire stellar population in the starburst; it represents the ‘net’ reddening, which includes the effects of both dust geometry and composition. It mostly describes dust absorption, since the effects of scattering are averaged out by the fact that we are observing the entire starburst, and therefore scattering out of the line of sight is compensated by scattering into the line of sight. In this light, the comparison of the starburst reddening curve with the extinction curves of Figure 1b is purely illustrative.

Two characteristics of the reddening curve are immediately apparent in Figure 1b. First, the curve lacks the 2200 Å bump of the Milky Way or LMC extinction curves. Second, it has a much shallower UV-optical slope than the other curves. The first characteristic has been

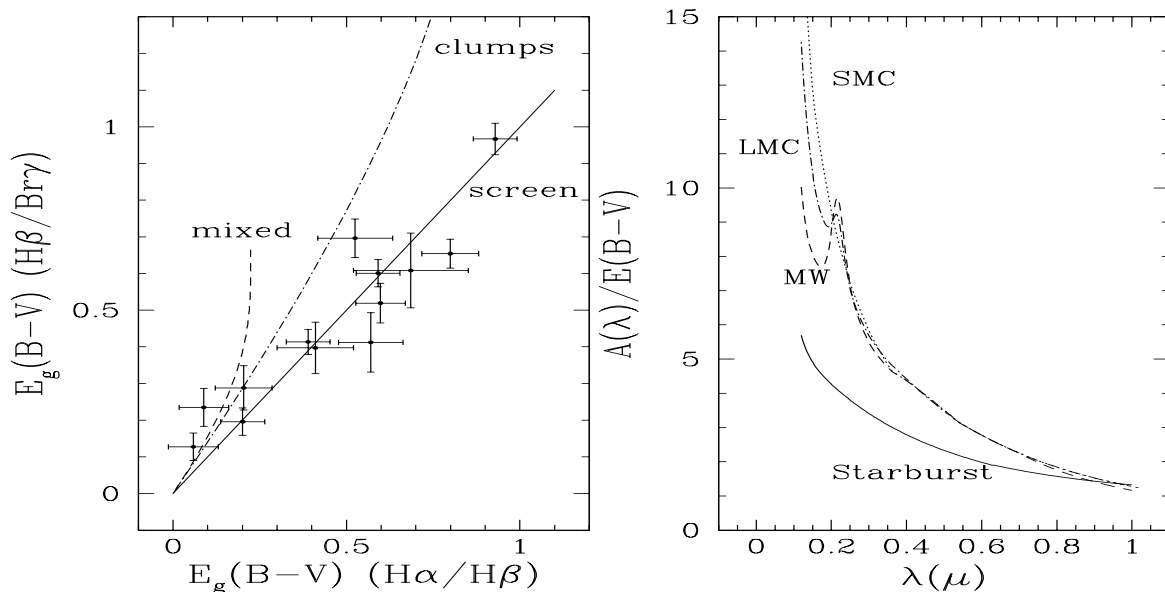


Figure 1: **(a)** (left): The color excess $E_g(B-V)$ derived from the hydrogen line ratio $H\beta/Br\gamma$ as a function of the same quantity derived from the ratio $H\alpha/H\beta$. The error bars are 1σ uncertainties. The data are compared with three models for the dust distribution: a homogeneous foreground *screen*; a *clumpy* foreground layer with an average of $\mathcal{N}_{\downarrow\uparrow\uparrow\downarrow} = 10$ along the line of sight; and a homogeneous *mixture* of dust and gas, which simulates the case of internal dust. For small $E_g(B-V)$, i.e. small reddening values, the models are degenerate; however, large $E_g(B-V)$ can be explained only by the foreground distributions (homogeneous and clumpy). Clumpy dust geometries with more than 10 clumps along the line of sight lay between the continuous and dot-dashed lines. **(b)** (right): The *Starburst* reddening curve, derived from continuum-color vs. gas-reddening plots like those in Figure 2, is shown as a function of wavelength, and compared with the interstellar extinction curves of the Milky Way, of the 30 Dor region in the LMC, and of the SMC.

proven to be intrinsic to the *extinction* curve of starbursts (Gordon, Calzetti & Witt 1997). No dust geometry is able to ‘wash away’ the bump if it is present in the extinction curve; thus the intrinsic extinction curve of starbursts must resemble the ‘bump-less’ SMC curve. The second characteristic is a combined effect of dust geometry and age segregation of the stellar populations (Calzetti et al. 1997). The dust in the starburst is likely to be clumpy, with the young, ionizing stars closely associated with the dust clumps. Stars are born in dusty molecular clouds, and the youngest stars have not had enough time to move away from the parental cloud. Conversely, the old, non-ionizing stars have lived long enough to migrate from their birth site and spread across the starburst region, filling also the dust-free interclump regions. Only the young stars ionize the gas, while both young and older stars contribute to the UV-optical continuum emission from the starburst. Therefore, the emission from the dust-associated gas is more reddened than the integrated UV-optical stellar continuum, resulting in a shallow reddening curve for the stellar population. This picture is a somewhat simplified description of what happens in a starburst, but has the power to provide a physical understanding of the observational evidence.

The reddening curve discussed in this section is an effective tool for removing the dust effects from the emerging light of starbursts. It has been derived entirely from observations and is totally model-independent. In addition, it can be used in the same way as standard extinction curves, in that the attenuation of the stellar continuum is given by: $A_{star} = E_g(B-V) k_{starburst}(\lambda)$. It should be stated again that this is only a convenient representation and does not imply that

the dust affecting the stellar continuum is in a foreground homogeneous screen. The reddening curve of Figure 1b is generally applicable to starburst regions, but not to subsonic HII regions or to quiescent galaxies.

The effects of dust on local, UV-bright starburst galaxies can be summarized as follows: the median attenuation at 1600 \AA is 1.6 mag, and at $H\alpha$ is ~ 0.8 mag. These numbers are important because star formation rates derived from the *observed* UV flux will be generally underestimated by a factor ~ 5 (and this sample is UV-selected!), while the same rates derived from the $H\alpha$ flux will be underestimated by a factor of 2. Even worse, about 30% of the young stars in this UV-bright sample are completely buried in dust and do not contribute either to the UV emission or to the nebular lines (Calzetti et al. 1995).

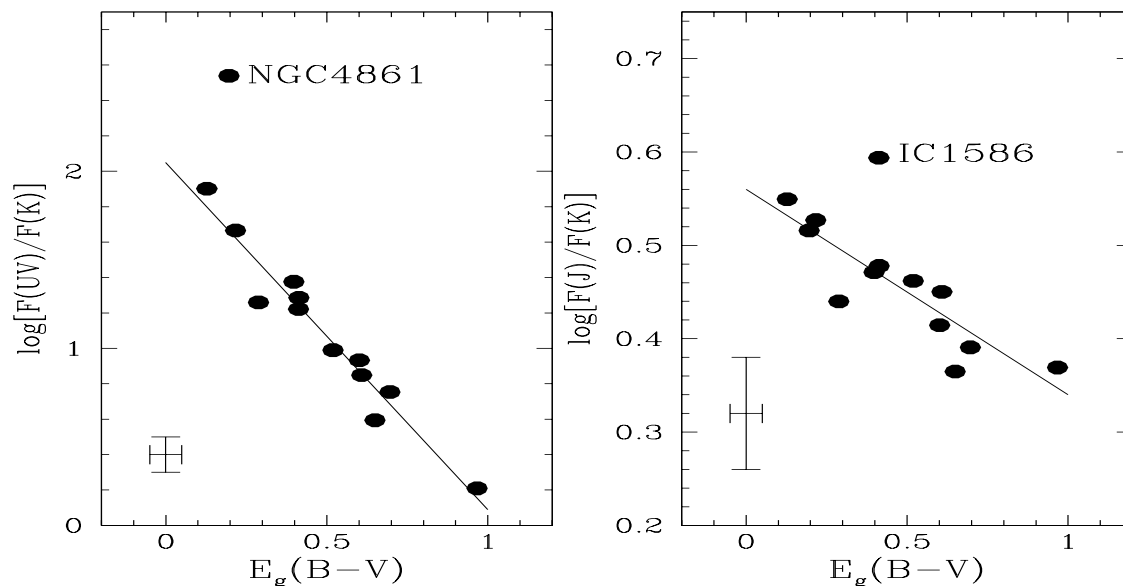


Figure 2: The observed UV–K (left panel) and J–K (right panel) colors of starbursts correlate with the reddening of the ionized gas, $E_g(B-V)$. The correlation indicates that the observed continuum colors are dominated by the effects of dust reddening, rather than variations in the intrinsic stellar populations. These and other similar correlations have been used by Calzetti et al. (1994) and Calzetti (1997) to derive the starburst reddening curve of Figure 1b. The 1σ uncertainties on the data points are indicated in the lower left corners of the two panels. The starburst galaxies NGC4861 (left panel) and IC1586 (right panel) deviate from the general trend set by the other galaxies. The deviation of NGC4861 is due to its much younger stellar population relative to the average; for IC1586 the culprit are the large photometric uncertainties (Calzetti 1997).

4 The Evolution of Dust Opacity

The increasing number of intermediate and high redshift galaxies which are being secured (e.g. Lilly et al. 1996, Steidel et al. 1996) have led to the first attempt to measure the evolution of the galaxy light density in the Universe. An extensive work was done by Lilly et al. (1996) who collected and used the CFRS data to derive the galaxy luminosity density in the redshift range $0 \leq z \leq 1$. Madau et al. (1996 and 1998) and Connolly et al. (1997) extended the plot by Lilly et al. to the redshift range $1 \leq z \leq 4$, using the HDF data (Williams et al. 1996). Adopting an average star formation history for the galaxies and a stellar initial mass function (IMF), Madau et al. (1996) converted the UV light density into a global star formation rate (SFR).

A number of authors have, however, warned against the danger of using the *observed* UV flux density as an indicator of SFR, because of its sensitivity to dust obscuration (e.g. Meurer et al. 1997, Rowan-Robinson et al. 1997). Although observations are being obtained to try to quantify the effects of dust obscuration at high redshift (e.g., Pettini et al. 1998), the issue is far from being a simple one because of the potential degeneracy of UV/optical indicators (see the discussion in Meurer, Heckman & Calzetti 1998).

For the reasons given in Section 1.2, the low metallicity of high redshift galaxies does not necessarily imply low dust opacities. To test this statement, one can attempt to follow the history of the metal and dust enrichment of galaxies using as zero-order approximation the SFRs derived from the *observed* UV flux densities as a function of redshift. Star formation implies metal and dust production, which can be converted into opacities with an educated guess on the dust geometry. The derived dust opacities are then used to correct the observed UV flux densities for the effects of dust obscuration, so that new values of the SFR can be obtained. This procedure is then repeated until the derived UV opacities and the ratio of observed-to-corrected UV flux densities converge to the same value (Calzetti & Heckman 1998). The convergence of the method is ensured by the fact that the increase in the global SFR leads to a faster consumption of the available gas and, although also the metal production increases, the general effect is to decrease the opacities, which therefore get closer in value to the corrected-to-observed UV ratio. Outflows/inflows are used to control the metal enrichment of the galaxies, which we impose to have a final gas metallicity $Z_{gas}=Z_{\odot}$.

Other authors (e.g. Pei & Fall 1995) have discussed the impact of dust obscuration in models of chemical enrichment of the Universe; this is the first time, however, that the *observed* SFR is used in an iterative procedure to derive the *intrinsic* SFR.

Assumptions on the model are that $\sim 10\%$ of the baryons are in galaxies; that merging is not a major galaxy formation process; that the half light radius of the galaxies increases with time (Giavalisco et al. 1996); that the stellar IMF is constant in time and with a Salpeter slope in the range $0.35\text{--}100 M_{\odot}$, with no stars formed below $0.35 M_{\odot}$; that instantaneous mixing holds for the metals and dust in galaxies; that the outflows/inflows are proportional to the SFR (Pei & Fall 1995); that the metal/dust ratio evolves with metallicity (Pettini et al. 1997); that the dust is homogeneously mixed with the stars (Xu & Buat 1995, Wang & Heckman 1996). The UV flux density at $z=4$ (Madau et al. 1998) is not included in the iterative procedure because, to date, there are only a few candidates which have been confirmed at that redshift, and volume corrections are currently unknown (Dickinson 1998, private communication). The uncertainty on the $z=4$ point is potentially large.

The observational constraints to the solutions are, in addition to the observed UV flux density as a function of redshift, the local dereddened $H\alpha$ energy density (see Gronwall 1998, these Proceedings; Gallego 1998, these Proceedings), the local FIR density (Soifer & Neugebauer 1991, Villumsen & Strauss 1987), and the Cosmic Infrared Background from COBE (CIB; Fixsen et al. 1998, Hauser et al. 1998).

Given the limited amount of observational constraints and the associated uncertainties, the method converges to multiple solutions, two of which (Figure 3a) represent extreme behaviors in the allowed range. One of the two solutions (Model 2) reproduces relatively well all observational constraints, except the CIB at long wavelengths (Figure 3b). Model 2 implies a modest dust correction, a factor $\times 2$, to the UV flux densities at $z > 2$ and a larger factor, $\sim \times 4$, at $z < 1$. The total amount of stars produced by this solution is modest enough that no outflows/inflows are required to keep the final gas metallicity to Z_{\odot} ; the solution actually produces a final gas metallicity $3/4 Z_{\odot}$. Model 2 has a peak at $z \sim 1$ and its shape closely resembles that of the observed SFR (Model 1 in Figure 3a).

The other solution, Model 3 (Figure 3a), reproduces the observational constraints, includ-

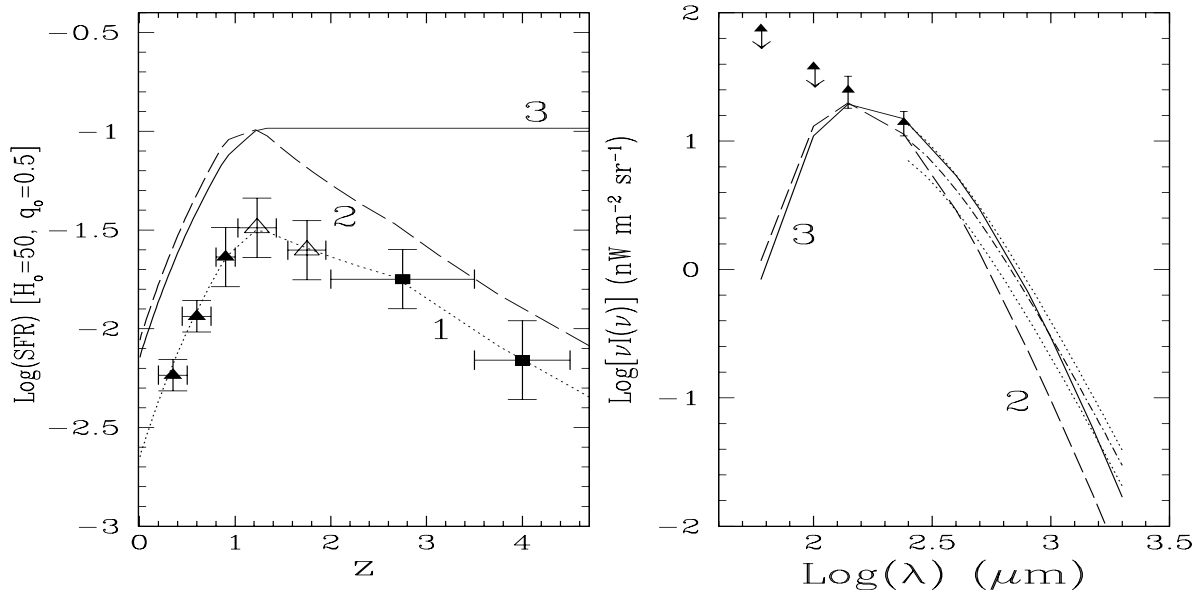


Figure 3: **(a)** (left) The global star formation rate as a function of redshift (Madau et al. 1996), renormalized to the adopted stellar IMF. The data points are from the observed UV flux densities reported by Lilly et al. (filled triangles), Connolly et al. (1997), and Madau et al. (1998). Model 1 is a smooth representation of the ‘observed’ SFR. Models 2 and 3 are the solutions of the iterative process described in the text. **(b)** (right) The Cosmic Infrared Background observed by COBE is compared with the predictions from the Models. The DIRBE data (Hauser et al. 1998) are represented by triangles with their 1σ uncertainty; the values at 60 and 100 μm are upper limits. The FIRAS data (Fixsen et al. 1998) are shown as a smooth curve (dot-dashed line) and its 1σ uncertainty (dotted curves). The prediction from the Models are shown as the continuous curve (Model 3) and the long-dashed curve (Model 2).

ing the long wavelength regime of the CIB (Figure 3b), better than Model 2. Modest outflows/inflows are required for this solution, implying that galaxies were in the past a factor $\sim 1.7/1.5$ heavier/lighter, respectively, than today. The UV dust reddening correction is $\times 3.2$ at $z < 1$ and greater than $\times 5$ at $z > 2$. The shape of Model 3 resembles the ‘monolithic collapse’ scenario for star formation. In Model 3, $\sim 20\%$ of the stars formed at $z > 3$.

Although Model 3 meets the observational constraints better than Model 2, current uncertainties, especially at high redshift, do not allow us to accept or reject altogether either of the solutions. It is, however, noteworthy that even in the most favorable case metal enrichment implies a dust correction factor of at least 2, and most likely as large as a factor of 5–6, on the observed UV flux densities and, therefore, on the global SFR at $z > 2$.

5 Summary

Low redshift galaxies are probably not very opaque: multiwavelength measurements indicate that the fraction of light absorbed by dust is about $1/2$, and no more than $2/3$, of the total stellar light. In the case of actively star-forming regions, a general tool is available to correct the observed UV/optical/near-IR emission for the effects of dust obscuration and, thus, recover the intrinsic flux.

High redshift data are still insufficient to answer the question of how much opaque young galaxies are. Estimates range from about $1/2$ to about $9/10$ of the total stellar light lost

to dust absorption. Simulations of the evolution of the dust content and opacity of galaxies suggest that, in the most optimistic case, about 1/2 of the light is lost to dust absorption at $z > 2$. However, the most optimistic case may not be the most likely one, and larger values of the opacity are possible at high redshift. Far-infrared observations more sensitive than those provided by ISO are needed to unambiguously address this issue.

Acknowledgements. The author gratefully acknowledge the Conference organizers and the STScI DDRF for providing financial support.

References

- [1] Aitken, D.K., Roche, P.F., Allen, M.C., & Phillips, M.M., 1982, *MNRAS* **199**, 31P
- [2] Berlind, A.A., Quillen, A.C., Pogge, R.W., & Sellgren, K. 1997, *Astron. J.* **114**, 107
- [3] Bianchi, L., Clayton, G.C., Bohlin, R.C., Hutchings, J.B., & Massey, P. 1996, *Astrophys. J.* **471**, 203
- [4] Calzetti, D. 1997, *Astron. J.* **113**, 162
- [5] Calzetti, D., Bohlin, R.C., Kinney, A.L., Storchi-Bergmann, T., & Heckman, T.M. 1995, *Astrophys. J.* **443**, 136
- [6] Calzetti, D., & Heckman, T.M. 1998, *Astrophys. J.* *submitted*,
- [7] Calzetti, D., Kinney, A.L., & Storchi-Bergmann, T. 1994, *Astrophys. J.* **429**, 582
- [8] Calzetti, D., Kinney, A.L., & Storchi-Bergmann, T. 1996, *Astrophys. J.* **458**, 132
- [9] Calzetti, D., Meurer, G.R., Bohlin, R.C., Garnett, D.R., Kinney, A.L., Leitherer, C., & Storchi-Bergmann, T. 1997, *Astron. J.* **114**, 1834
- [10] Cardelli, J.A., Clayton, G.C., & Mathis, J.S. 1989, *Astrophys. J.* **345**, 245
- [11] Connolly, A.J., Szalay, A.S., Dickinson, M., Subbarao, M.U., & Brunner, R.J. 1997, *Astrophys. J.* **486**, L11
- [12] Fixsen, D.J., Dwek, E., Mather, J.C., Bennett, C.L., Shafer, R.A. 1998, *Astrophys. J.* *in press*,
- [13] Giavalisco, M., Steidel, C.C., & Macchetto, F.M. 1996, *Astrophys. J.* **470**, 189
- [14] Giovanelli, R., Haynes, M.P., Salzer, J.J., Wegner, G., Da Costa, L.N., & Freudling, W. 1995, *Astron. J.* **110**, 1059
- [15] Gonzalez, R.A., Allen, R.J., Dirsch, B., Ferguson, H.C., Calzetti, D., & Panagia N. 1998, *Astrophys. J.* *in press*,
- [16] Gordon, K.D., Calzetti, D., & Witt, A.N., *Astrophys. J.* **487**, 625
- [17] Gordon, K.D., & Clayton, G.C. 1998, *Astrophys. J.* *in press*,
- [18] Hauser, M.G., *et al.* 1998, *Astrophys. J.* *in press*,
- [19] Heckman, T.M., Armus, L., & Miley, G. 1990, *Astrophys. J. Suppl. Ser.* **74**, 833
- [20] Jones, A.P., Tielens, A.G.G.M., Hollenbach, D.J., & McKee, C.F. 1994, *Astrophys. J.* **433**, 797
- [21] Kennicutt, R.C. 1989, in *Massive Stars in Starbursts*, p. 157, eds. Leitherer, Walborn, Heckman and Norman, Cambridge Univ. Press
- [22] Leitherer, C., & Heckman, T.M. 1995, *Astrophys. J. Suppl. Ser.* **96**, 9
- [23] Lilly, S.J., Le Fèvre, O., Hammer, F. & Crampton, D. 1996, *Astrophys. J.* **460**, L1

- [24] Madau, P., Ferguson, H.C., Dickinson, M.E., Giavalisco, M., Steidel, C.C., & Fruchter, A. 1996, *MNRAS* **283**, 1388
- [25] Madau, P., Pozzetti, L., & Dickinson, M. 1998, *Astrophys. J.* **498**, 106
- [26] Meurer, G.M., Heckman, T.M., & Calzetti, D. 1998, *in preparation*
- [27] Meurer, G.R., Heckman, T.M., Leitherer, C., Kinney, A.L., Robert, C., & Garnett, D.R. 1995, *Astron. J.* **110**, 2665
- [28] Meurer, G. R., Heckman, T.M., Lehnert, M.D., Leitherer, C., & Lowenthal, J. 1997, *Astron. J.* **114**, 54
- [29] Natta, A., & Panagia, N. 1984, *Astrophys. J.* **287**, 228
- [30] Pei, Y.C., & Fall, S.M. 1995, *Astrophys. J.* **454**, 69
- [31] Pettini, M., Kellogg, M., Steidel, C.C., Dickinson, M., Adelberger, K.L., & Giavalisco, M. 1998, *Astrophys. J.* **submitted**,
- [32] Pettini, M., King, D.L., Smith, L.J., & Hunstead, R.W. 1997, *Astrophys. J.* **478**, 536
- [33] Rowan-Robinson, M., et al. 1997, *MNRAS* **289**, 490
- [34] Sandage, A., Saha, A., Tamman, G.A., Labhardt, L., Schweneler, H., Panagia, N., & Macchetto, F.D. 1994, *Astrophys. J.* **423**, L13
- [35] Soifer, B.T., & Neugebauer, G. 1991, *Astron. J.* **101**, 354
- [36] Steidel, C.C., Giavalisco, M., Pettini, M., Dickinson, M., & Adelberger, K.L. 1996, *Astrophys. J.* **462**, L17
- [37] Villumsen, J.V., & Strauss, M.A. 1987, *Astrophys. J.* **322**, 37
- [38] Wang, B., & Heckman, T.M. 1996, *Astrophys. J.* **457**, 645
- [39] White, R.E., Keel, W.C., & Conselice, C.J. 1996, *preprint* (astroph/9604029)
- [40] Williams, R.E., et al. 1996, *Astron. J.* **112**, 1335
- [41] Witt, A.N., Thronson, H.A., & Capuano, J.M. 1992, *Astrophys. J.* **393**, 611
- [42] Witt, A.N., & Gordon, K.D. 1996, *Astrophys. J.* **463**, 681
- [43] Xu, C., & Buat, V. 1995, *Astr. Astrophys.* **293**, L65